Neural Computing and Applications (2021) 33:591–602
https://doi.org/10.1007/s00521-020-04987-4

S.I. : DPTA CONFERENCE 2019

Application of artificial neural network model based on GIS in geological hazard zoning

Qulin Tan[1,2] · Yong Huang[3,4,5,6] · Jun Hu[7] · Pinggen Zhou[8] · Jiping Hu[1,2]

Received: 17 February 2020 / Accepted: 2 May 2020 / Published online: 27 June 2020
© Springer-Verlag London Ltd., part of Springer Nature 2020

Abstract

Under specific terrain and climatic conditions, it is extremely easy to cause various types of geological hazards, and the occurrence of geological hazards will affect people's production and life, with the consequence that the economic losses are extremely great, and even severely endanger human life. However, the existing geological hazard danger zoning is slightly insufficient in accuracy and operating efficiency, and the effect in practical application needs to be further improved. In view of the above problems, this paper proposes a study on the application of GIS-based artificial neural network models in the geological disaster risk zoning. This article first expounds the related concepts of geological hazards zoning and gives the principles to be followed. Then, the calculation of evaluation factors and risk level probabilities are proposed, and a hierarchical model is constructed using the analytic hierarchy process. The weight of each evaluation factor is multiplied with the information to obtain the weighted information. Calculate the probability based on the topographic features, stratigraphic lithology, and terrain slope. Combine the artificial neural network with BP neural network to predict the results. Through the simulation experiments on the geological data of the low-mountain and hilly areas in Wanli District, Nanchang, the results show that the proportion of high-probability-prone areas and medium-probability-prone areas predicted by this paper is as high as 91.87%, and the evaluation results are consistent with the actual disaster occurrence better. The area under the ROC curve was 87.3%, which also verified the effectiveness of the method in this paper.

Keywords Geological hazard risk zoning · Geographic information system (GIS) · Artificial neural network · Danger level probability

✉ Yong Huang
memtrudi602@student.citruscollege.edu

Qulin Tan
qltanbjtu@163.com

Jun Hu
junhu@m.bjtu.edu.cn

Pinggen Zhou
zhoupg@cigem.cn

Jiping Hu
jphu@bjtu.edu.cn

[1] School of Civil Engineering, Beijng Jiaotong University, Beijing 100044, China

[2] Institute of Spatial Information for Line Engineering, Beijng Jiaotong University, Beijing 100044, China

[3] Xinjiang Communication Construction Co. Ltd. (XCCG), Urumqi 830000, Xinjiang, China

[4] Chengdu University of Technology, Chengdu 610000, Sichuan, China

[5] Transpotation Industry Highway Maintenance Collaborative Innovation Platform Under Complicated Conditions of Western China, Urumqi 830000, Xinjiang, China

[6] Western Sub-Alliance of Zhongguancun Zhongke Highway Maintenance Technology Innovation Alliance, Urumqi 830000, Xinjiang, China

[7] School of Computer and Information Technology, Beijng Jiaotong University, Beijing 100044, China

[8] China Institute of Geo-environment Monitoring, Ministry of Natural Resources, Beijing 100081, China

1 Introduction

As a catastrophic event, geological disasters will lead to casualties and property damage or damage the ecological environment [1]. This catastrophic event is caused by the mutual influence and interaction of natural geological or man-made geological environment or geological subject in the hydrosphere, atmosphere and biosphere on the surface of the earth's lithosphere crust [2]. Once a geological disaster occurs, the consequences are unthinkable, social production and life are affected, the ecological environment is damaged, and the human physiological and psychological state will be damaged to varying degrees, and even endanger life. According to reports, the losses caused by various geological disasters are enormous [3]. China's annual economic losses caused by various disasters are as high as 13–14 billion yuan [4]. At present, promoting the mitigation of geological disasters has become a hot issue for all sectors of society and countries [5]. The process of geological hazards is very complicated. The study of the danger zoning of geological hazards will help improve the accuracy of geological hazard predictions and reduce the losses caused by geological hazards.

In terms of geological hazard prediction and forecasting, geological hazard danger zoning is an important research direction, and many scholars have conducted research and achieved fruitful results. In [6], the author points out that 12.6% of the land on the Indian subcontinent is susceptible to landslide disasters, and the total economic loss due to landslide disasters is estimated to be 4,500,000 US $. The author describes the spatiotemporal development of different methods of landslide disaster zoning and their advantages and disadvantages and finds that knowledge-driven and bivariate analyses have been most commonly used in the past decade. But since the twentieth century, multivariate statistical models have been widely used because it provides the most accurate zoning results of landslide disasters compared to other methods. In [7], the author simulated the effects of uplift and topographical precipitation on the evolution of orogenic belts through an empirical model, and estimated it as a trend of excavation rate by means of thermochronology. Based on morphological structure and sedimentological analysis, the channel changes narrowness and increased sediment eventually lead to flooding. In [8], the author used the seismic catalogue of 16°–24° N latitude and 67°–86° latitude from 1502 to 2012 as the data source and calculated it using a 16-arm logical tree of the ground motion prediction equation. The UHS chart presents the results of earthquake hazard prediction. In [9], the author estimates the risk of earthquake landslides in the syntax area of the Himalayas in the eastern Tibetan Plateau. The eastern Himalayan grammar area is one of the most active tectonic activities on the earth and the most prone to earthquakes. Frequent earthquakes and geological disasters in this area have caused huge damage. Based on the analysis of seismic geological background and field investigation, the author first considered the effects of river erosion, active faults and seismic amplification, and used the Newmark method to draw a seismic landslide disaster map with a PGA exceeding probability of 10%. In [10], the author selected a grid of 1 km × 1 km as the evaluation unit to show the spatial distribution of landslide risk in China. A combination model of deterministic factor model and logistic regression model was used to evaluate the landslide disaster. The Liu's method was used to assess the landslide vulnerability and product hazard times vulnerability ratios to represent the landslide risk. In [11], the authors developed a landslide sensitivity and hazard map using the adaptive univariate value analysis (VABU) method for the Nahr Ibrahim watershed in Mount Lebanon. In [12], the author conducted a probabilistic earthquake disaster assessment on Sulawesi, Indonesia, which included the effects of site amplification, and found that high seismic activity rates in distributed deformation areas can cause great danger. In [13], the authors evaluated the landslide disaster zoning triggered by two Akhal-Walleighan earthquakes using multilayer perceptrons and Gaussian radial basis functions. In [14], the author proposed a GIS-based landslide disaster assessment and zoning based on the Yildu district in central Ethiopia. In [15], the authors considered the geological and geomorphological factors of natural disasters in the Carpathian region of Ukraine and established a conceptual model. The weight coefficients of potential landslide-prone factors were determined by field observations and archive data. Finally, a complete space map of landslide sensitivity is presented. The above studies have achieved good results in geological disasters, but there are still many shortcomings. First, in some studies, although GIS technology was used to establish a geological database, it was not possible to further analyze and evaluate it, so that it was difficult to achieve the results of dangerous zoning. Second, the method of artificial evaluation and analysis is not effective and has the problem of low efficiency. It is easy to cause deviations in the obtained results due to the existence of prior experience.

The classification of geological hazards is a complex and fuzzy processing event [16]. GIS technology can be used to build a geological database, and artificial neural networks are characterized by nonlinear parallel processing to process information that is fuzzy, complex, highly random, and large in volume [17, 18]. Therefore, combining GIS technology with artificial neural network may achieve unexpected results. Artificial neural networks have applications in many fields. In [19], the author used artificial

neural networks to solve the quantum multibody problem, and achieved high accuracy when describing the one-dimensional and two-dimensional prototype interaction spin models. In [20], the author applied artificial neural networks to IoT devices, providing them with ultra-reliable low-latency communication and extensive connections. In [21], the author used artificial neural networks for olive oil production, so that the authenticity, sensory characteristics, and other quality-related characteristics of olive oil were also tested. In [22], the author used artificial neural networks to optimize the copper(II) biosorption in sea urchin experiments and found that the optimal copper removal efficiency of the biosorbent was 89.09%. In [23], the authors used artificial neural networks for large-scale, high-resolution comparison of core visual object recognition behavior. In [24], the author applied artificial neural networks to the prediction of English letters, and the prediction accuracy was greatly improved. In [25], the author applied artificial neural networks to select high-quality students for MBA courses in business schools to achieve the target employment rate. In [26], the authors used artificial neural networks to predict the performance of heat pump water heaters, and the prediction results were in line with reality. One of the most important research topics in smart grid technology is load forecasting, because the accuracy of load forecasting will greatly affect the reliability of smart grid systems. In [27], the author applied the artificial neural network to the coincidence prediction of the smart grid. The cumulative changes of the average absolute percentage error and the root-mean-square error of the algorithm were 9.77% and 11.66%, respectively. In [28], the author applied artificial neural network to stiffness estimation in magnetic resonance elastography, which has the advantage of being more resistant to noise. In summary, artificial neural networks have obvious advantages in dealing with fuzzy and complex problems, and they can effectively perform predictive analysis. Therefore, it is considered to combine GIS technology with artificial neural network for the study of geological disaster risk zoning.

Aiming at the problems of the existing geological disaster risk zoning methods with poor accuracy and operational efficiency, this paper proposes a study on the application of GIS-based artificial neural network models in geological disaster risk zoning. This article takes slope, height difference, engineering geological rock and soil types, human engineering activities as evaluation factors. A hierarchical model is constructed using the analytic hierarchy process. The weight of each evaluation factor is multiplied with the amount of information to obtain the weighted information amount, and the danger level probability is calculated, combined with BP neural network in artificial neural network for prediction. Through the simulation experiments of the geological data in the low-mountain and hilly area of Wanli District, Nanchang, GIS was used to perform grid coverage analysis on the weighted information amount of each impact factor to obtain a weighted information amount distribution map, and reclassify them at equal intervals. Finally, the study area is divided into four levels: high-probability-prone areas, medium-probability-prone areas, low-probability-prone areas, and non-prone areas. The proportion of high-probability-prone areas and medium-probability-prone areas predicted by this paper is as high as 91.87%, and the evaluation results agree well with the actual disaster occurrence. The area under the ROC curve was 87.3%, which also verified the effectiveness of the method in this paper. In the prediction of BP neural network, the accuracy rate of the grid weight matrix prediction tends to increase as the number of training times increases, and the final prediction accuracy rate is as high as 90%.

2 Geological hazard risk assessment

2.1 Concepts related to geological hazard zoning

Geological hazard danger zone belongs to the scope of geological hazard spatial prediction. In other words, based on the research on the development status and formation mechanism of geological disasters, the main factors that control and influence the formation of geological disasters are selected. In addition, a method is used to estimate the possibility of potential geological hazards in the future and to complete the geological hazard risk prediction zoning. The ultimate purpose of geological disaster risk zoning supported by GIS is to divide regions of different disaster levels and reflect them through disaster maps to provide a basis for early warning of geological disasters. Mathematically speaking, the division of geological disasters is a surveying and mapping process. For the danger of geological disasters, the degree of stability of the geological body is used here to describe. Geological disaster zoning mainly considers the basic factors that control and influence the occurrence of geological disasters and their contribution to the stability of the system. They are superimposed and combined according to some mathematical methods to determine the level of stability or danger at the geological body level. Geological hazards are classified based on major hazard indicators. In this process, we should give full consideration to the "people-oriented" thinking. Comprehensively consider the development status, development trends and many factors affecting the development of geological hazards. The following principles should be followed:

(1) Dominant factor and factor comparison principle

The occurrence of geological disasters is the result of various environmental factors in the natural environment. There are various types of environmental factors included, such as topography, forest vegetation, geological structure, stratigraphic lithology, rainfall, and even people's production and life. These factors interact and influence each other. Among these factors, there are leading factors that determine the combined characteristics and degree of danger of geological hazards to a large extent. However, some factors are comparable in time distribution, but the law of comparability in spatial distribution is weak. These are nonmain factors. In the study, it is necessary to comprehensively analyze each factor and grasp the main factors.

(2) The principle of relative consistency

In the same category, the development degree and triggering factors of geological hazards should have the greatest similarity, and there should be obvious differences in different categories, so that the geological hazard zoning is meaningful.

(3) Scientific and practical principles

Scientificity mainly means that the proposed method must have a theoretical basis to ensure the reliability of the data and the feasibility of the zoning level. The practicability is mainly to highlight that the method is easy to implement and the division results are simple and easy to understand.

(4) Principle of qualitative and quantitative combination

The natural environment is very complex, and there are ambiguities between regions. Its changes are difficult to describe with mathematical formulas, so it cannot be completely studied by quantitative methods. Based on the qualitative analysis, the development laws of geological disasters are summarized, and their similarities and differences are distinguished. Then use quantitative methods to reflect the relationship between geological disasters and various factors, and reflect the real situation through a combination of qualitative and quantitative.

(5) The principle of combining type zoning and comprehensive zoning

The type zone reflects the risk level of different units. However, geological hazards are very complex and diverse. In the process of division, we must understand the geological data from various aspects and transform according to the actual situation, so that we can build a model close to the actual.

2.2 Geological hazard risk assessment factors and risk level probability

(1) Selection of evaluation factors and determination of weight

According to the development characteristics and distribution rules of geological hazards, the consideration of evaluation factors mainly includes slope, height difference, engineering geological rock and soil types, geological structures, slope structure types, and human engineering activities. Divide the grid unit of 30 m by 30 m as the smallest unit. The hierarchical structure model is established by using the analytic hierarchy process, and the index weight is obtained after normalizing the vector. The weighted information amount is obtained by multiplying the weight of each evaluation factor with the information amount. The calculation process is as follows:

(1) Calculate the amount of information provided by each factor x_i on the geological disaster event L:

$$I(L, x_i) = \ln \frac{N_i/N}{S_i/S} \tag{1}$$

In the above formula, S represents the total number of evaluation units in the area under study, and N is the number of units for geological hazard distribution. S_i is the number of units in the study area that contains the evaluation factor x_i, and N_i is the number of units of a particular category of geological hazards distributed within the factor x_i.

(2) Calculate the total amount of information in a single grid:

$$I = \sum_{i=1}^{n} I_i = \sum_{i=1}^{n} \ln \frac{N_i/N}{S_i/S} \tag{2}$$

(3) Calculate the total weighted information in a single grid:

$$I_w = \sum_{i=1}^{n} W_i \cdot \ln \frac{N_i/N}{S_i/S} \tag{3}$$

In the above formula, W_i indicates the weight value of the ith evaluation factor, I indicates the total information amount of the evaluation unit, and I_w indicates the total weighted information amount of the evaluation unit. The larger the value, the greater the possibility of geological disasters in the unit.

(2) Calculation of risk level probability

Dividing the danger level requires calculating the probability of each grid topography, lithology, terrain slope danger and other indicators. Each risk probability is calculated as follows:

(1) Terrain and geomorphic danger probability $F_{topography}$

$$F_{topography} = x_1 f_{high} + x_2 f_{medium} + x_3 f_{low} + x_4 f_{river\ valley} \quad (4)$$

In the above formula, f_{high}, f_{medium}, f_{low}, and $f_{river\ valley}$, respectively, represent the probability of geological disasters in the high mountain, medium height mountain, low mountain, and river valley. The coefficients x_i $(i = 1, 2, 3, 4)$ in turn correspond to the areas occupied by different topographic features in a certain grid.

(2) Probability of formation lithology danger $F_{stratigraphic\ lithology}$

$$F_{stratigraphic\ litho\log y} = x_1 f_{carbonate} + x_2 f_{magmatic\ rock} + x_3 f_{metamorphic\ rock} + x_4 f_{gravel\ soil} \quad (5)$$

In the same way, the coefficient x_i $(i = 1, 2, 3, 4)$ corresponds to the area occupied by different stratigraphic lithologies in a certain grid in turn.

(3) Terrain slope danger probability $F_{terrain\ slope}$

$$F_{terrain\ slope} = x_1 f_1 + x_2 f_2 + x_3 f_3 \quad (6)$$

In the formula, f_1, f_2, f_3 represents the probability of disasters occurring under different slopes, and the corresponding slopes are x_1 (slope less than 10°), x_2 (slope between 10° and 25°), and x_3 (slope greater than 25°).

Synthesize the risk probability of the three factors to get the probability of geological hazard danger in a certain grid, that is:

$$P = N(F_{topography} + F_{stratigraphic\ litho\log y} + F_{terrain\ slope}) \quad (7)$$

In the above formula, P is the probability of the danger of geological hazards in a certain grid, and N is the number of disaster points that have occurred in a certain grid.

2.3 BP neural network model and principle

(1) BP neural network model

In this paper, BP neural network (i.e., back propagation neural network) in artificial neural network is used to help realize the geological disaster risk zoning. The BP neural network includes an input layer, a hidden layer, and an output layer. Neurons in adjacent layers are connected together, but neurons in each layer are discontinuous. The structure diagram of BP neural network is shown in Fig. 1.

In Fig. 1, $x_1(k), x_2(k), \ldots, x_n(k)$ represents the input of each element in the network input layer, and $y_1, y_2, \ldots, y_q$ represents the output of each element in the output layer.w_{ih} represents the connection weight between each element of the neural network input layer and each element of the network intermediate layer, and w_{ho} represents the connection weight between each element of the neural network intermediate layer and each element of the network output layer.

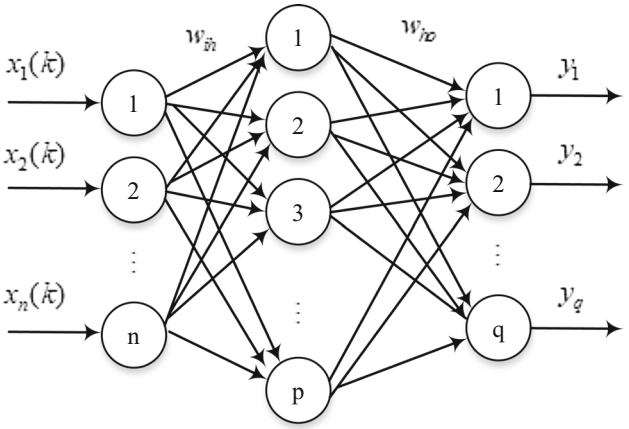

Fig. 1 Schematic diagram of the BP neural network

(2) Principle of BP neural network

The training of BP neural network has two links, which are the forward propagation of the signal and the backward propagation of the error. Taking the structure diagram shown in Fig. 1 as an example, based on this diagram, it is further assumed that the threshold values of each neuron in the hidden layer and the output layer are divided into b_h and b_o. The specific implementation steps of the BP neural network algorithm are as follows:

(1) Initialize the network

The first is the selection of two weights w_{ih} and w_{ho} and two thresholds b_h and b_o. Randomly select a number between -1 and 1 and not 0 as the initial value of the network. In addition, the initial learning rate η is set, and the activation function $f(s)$ of each neuron including the layer and the output layer is set, and the calculation accuracy value ε is set.

(2) Calculate the input $hi_h(k)$ of the hidden layer and the output $ho_h(k)$ of the hidden layer

The input of the hidden layer is obtained according to the input vector $x_n(k)$, the connection weight w_{ih} of the input layer element and the hidden layer element, and the connection threshold b_h.

$$hi_h(k) = \sum_{i=1}^{n} w_{ih} x_i(k) - b_h \quad (8)$$

In the above formula, $i = 1, 2, \ldots, n$, $h = 1, 2, \ldots, p$.

According to the input of the hidden layer $hi_h(k)$ and the activation function f, the output of the hidden layer is obtained. The calculation formula is as follows:

$$ho_h(k) = f(hi_h(k)) = f\left(\sum_{i=1}^{n} w_{ih}x_i(k) - b_h\right) \quad (9)$$

Since the geological hazard zoning in this paper is a nonlinear problem, the choice of activation function uses an S-shaped function with the following formula:

$$f(x) = \frac{1}{1+e^{-x}} \quad (10)$$

(3) Calculate the $yi_o(k)$ of the output layer and the output $yo_o(k)$ of the output layer

The calculation formulas for the input and output of the output layer are as follows:

$$yi_o(k) = \sum_{h=1}^{p} w_{ho}ho_h(k) - b_o \quad (11)$$

$$yo_o(k) = f(yi_o(k)) = f\left(\sum_{h=1}^{p} w_{ho}ho_h(k) - b_o\right) \quad (12)$$

In the above two formulas, $h = 1, 2, \ldots, p$, $o = 1, 2, \ldots, q$.

(4) Error calculation

The source of the error e is mainly due to the difference between the output of the network and the actual result data. This can be obtained from the actual output $yo_o(k)$ of the network and the expected output d_0 (k). It is calculated as follows:

$$e = \frac{1}{2}\sum_{o=1}^{q}(d_o(k) - yo_o(k))^2 \quad (13)$$

(5) Update weight

The error e is transmitted in the inverse direction of the network to all neurons in each layer to obtain their respective errors and to correct the weights w_{ih} and w_{ho} accordingly. It is calculated as follows:

$$W_{ho} = w_{ho} + \eta\{d_o(k) - yo_o(k)\}f'(yi_o(k)) \quad (14)$$

$$W_{ih} = w_{ih} + \eta\left\{\sum_{o=1}^{q}(d_o(k) - yo_o(k))f'(yi_o(k)w_{ho}\right\} \times f'(hi_h(k))x_i(k) \quad (15)$$

In the above formula, η represents the learning rate.

(6) Update threshold

The threshold b_h is updated by the error e. The calculation method of the two is as follows:

$$b_o = b_o + e \quad (16)$$

$$b_h = b_h + \left\{\sum_{o=1}^{q}(d_o(k) - yo_o(k))f'(yi_o(k)w_{ho}\right\} \times f'(hi_h(k)) \quad (17)$$

(7) Update learning times. The number of learning times is increased once and compared with a preset maximum number.

(8) Determine whether the error meets the requirements. If it does, the whole process ends, otherwise go to (2) continue to the next round of learning.

2.4 GIS combined with artificial neural network model applied to geological disaster risk zoning

When applying a combination of GIS and artificial neural network models to geological disaster risk zoning, first of all, a certain number of known samples are determined based on experience gained in previous research fields. According to different danger levels, with the support of GIS technology, it is divided into different collapse and landslide danger levels and quantified as the expected output of the output layer nodes. Use these already known samples to train the network until the total network error reaches the accuracy requirement. Then output the prediction result directly through the associative memory function of the neural network. The user can determine whether to relearn and adjust the opposite samples in the known samples based on the post-judgment and prediction results. Next, when the user is satisfied, write the prediction result in the corresponding field of the zone file and display it as a map.

The process of neural network evaluation and prediction model is shown in Fig. 2. The implementation part in the figure represents the learning process of the model, and the dashed part represents the model prediction process.

3 Evaluation index system

3.1 Data source and data processing

There are various factors leading to geological disasters, including internal factors and external factors. Internal factors are basically related to the geographical environment, such as ground slope and terrain. Most external factors are related to climate and humans, such as rainfall and human activities that change nature. Based on this, in this study, the low-lying hilly area of Wanli District, Nanchang City, Jiangxi Province was selected as the

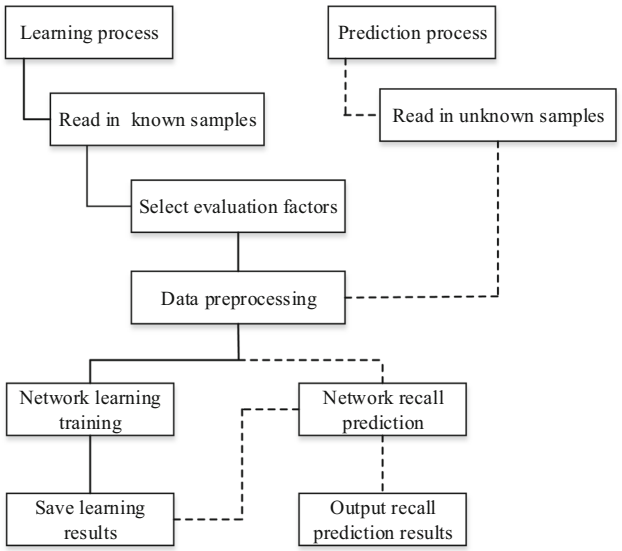

Fig. 2 Neural network evaluation prediction model

research object. The geological structure in this area is complex, and the weathering and fragmentation of rocks such as surface granite and metamorphic rocks are severe. According to statistics, so far, more than 80 geological disasters have occurred, and the types of disasters include problems such as collapse, mudslides, landslides, and ground subsidence. The selected data include GDEMV2 30 m resolution DEM data from the geospatial data cloud, and 1: 50,000 geological maps and geological disaster point data in Nanchang Wanli District.

3.2 Evaluation index system

The occurrence of geological disasters is caused by a variety of factors. To assess the occurrence of geological disasters, we must understand each of the small factors that make up these geological disasters. These factors mainly include geological environment, meteorological information, etc., and combine to establish an evaluation index system for evaluating the possibility of geological disasters. According to the provisions of the "Ministry of Land and Resources and China Meteorological Administration on Joint Development of Geological Hazard Meteorological Early Warning Work Agreement", the geological disaster meteorological forecast early warning levels are divided into five levels, as shown in Table 1.

By analyzing the geological environmental factors in the evaluation area, the probability of geological disaster danger in the area within the next 24 h from the meteorological department and the future rainfall information in the area were obtained. Combined with the actual rainfall in the previous period, the BP neural network fine grid model was used to provide early warning of geological hazards and predict the level of geological hazards in the evaluation area. Final disaster level and GIS technology for geological disaster risk zoning.

Table 1 Classification of meteorological forecast and early warning levels for geological hazards

Warning level	Possibility	Risk probability
1	Unlikely	< 0.1
2	Less likely	< 0.2
3	Likely	< 0.3
4	More likely	< 0.4
5	Very likely	> 0.4

4 Results and discussion

Result 1 Raster ratio and information amount of each evaluation factor

According to the characteristics and distribution of disasters in the low mountain and hilly area of Wanli District, Nanchang City, the evaluation factors such as the height difference of the mountain, the slope terrain, the type of rock and soil, and the human engineering activity are taken as examples to explain. The case ratio and information volume are as follows.

(1) Height difference

According to the actual situation of the mountain top and lake area, combined with the amount of information of each height difference interval, the height difference is divided into four intervals, which are 0–3 m, 3–6 m, 6–10 m, and 10–20 m. The amount of information is shown in Fig. 3.

It can be seen from Fig. 3 that in the studied area, the height difference that is most prone to geological hazards is 6–10 m, and the number of geological hazards in the unit is about 50.30%.

(2) Slope terrain

Slope is one of the important indicators reflecting the terrain of the slope. In steep slopes, the surface water runoff speed is fast, the surface erosion intensity is strong, and the sediment on the slope is easily deformed and unstable. Vegetation on steep slopes is not easy to grow, which is not conducive to the stability of the slope. However, in high-slope areas, loose materials are not easy to accumulate on slopes, and there is no material source for landslides. Generally, slope is an important factor influencing the occurrence of landslides. Here the slope is divided into four

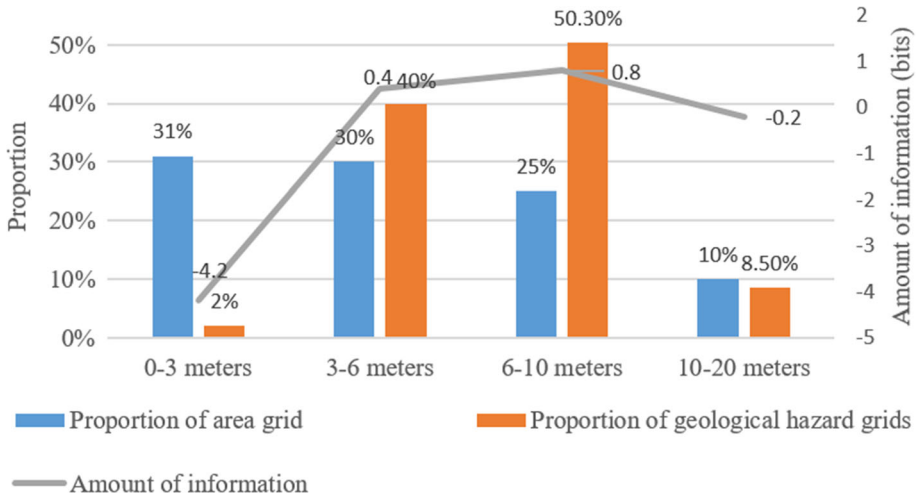

Fig. 3 Scale ratio and information value of each height difference interval

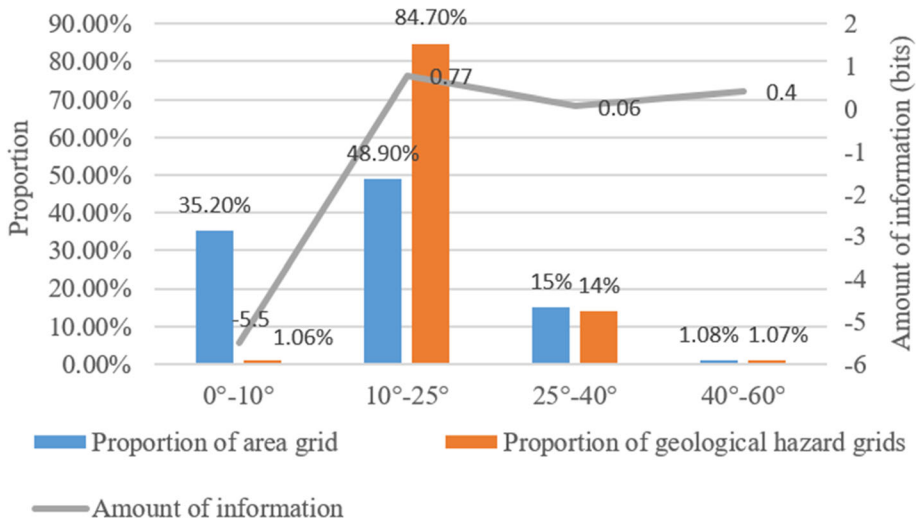

Fig. 4 Scale ratio and information amount of each gradient distribution

sections, which are 0°–10°, 10°–25°, 25°–40°, and 40°–60°. After the gradient classification, the information amount of the gradient distribution is further obtained, as shown in Fig. 4.

As for the slope, the most favorable geological hazards in the study area are 10°–25°. The number of grids accounts for 48.9% of the total grids, the proportion of geological hazards occurring is 84.7%, and the amount of information provided is 0.77.

(3) Rock and soil types

Rock and soil types are the material basis for geological disasters. Although various types of rocks may cause geological disasters, the contribution rates of different rocks and soil bodies to geological disasters are obviously different. The higher the mechanical strength and integrity of the rock, the lower the possibility of a geological disaster; the looser the rock and soil, the softer the lithology, the worse the interlayer cementation, and the higher the probability of a geological disaster. According to the soil characteristics of the study area and the actual situation, the rock and soil are divided into 5 types as shown in Fig. 5, which are: (a) loose rock group; (b) clastic engineering geological rock group; (c) harder to weaker layered sand and shale rock groups; (d) glutenite and quartz sandstone engineering geological rock groups; (e) karst limestone and marl with soft shale rock groups. It can be seen from the figure that group (b) (c) (e) is the most important type of rock and soil in the studied area, accounting for 93.1% of the total grid in the study area, and the proportion of geological disasters is 82.4%. This is most conducive to the occurrence of geological disasters.

(4) Human engineering activities

As for human engineering activities, there are mainly road construction and mountain development. According to the intensity of human engineering activities, the natural breakpoint method is divided into three levels. When the height of the excavated frontier is less than 3 m, the activity is weak, the height is between 3 and 10 m, and the

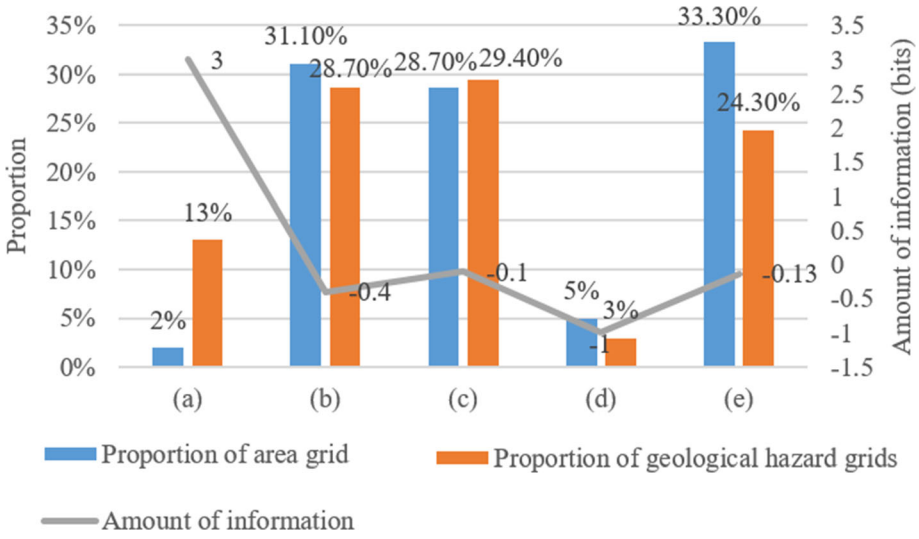

Fig. 5 Grid scale and information amount of engineering geological rock group

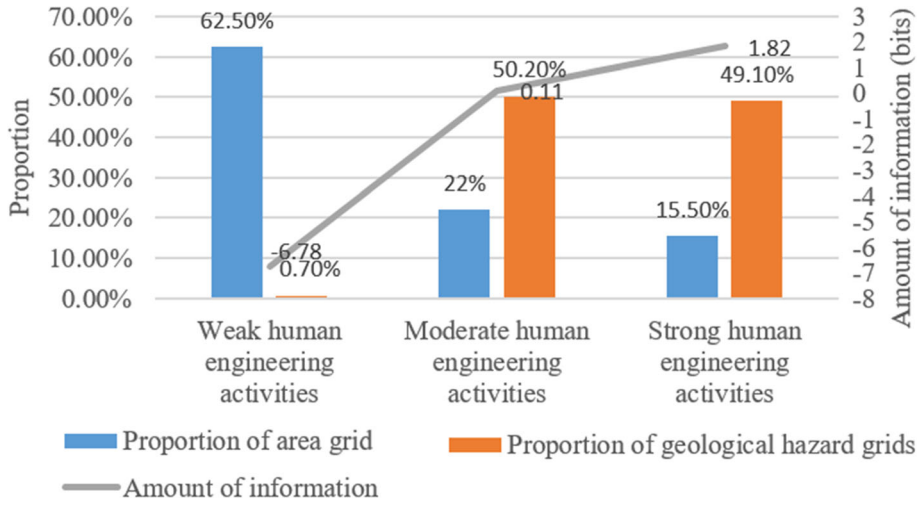

Fig. 6 Grid scale and information amount of human engineering activities

activity is moderate. The grid scale and information are shown in Fig. 6.

It can be seen from Fig. 6 that the human engineering activities are strong in moderate and severe geological disasters, accounting for 37.5% of the total grid in the study area, the proportion of geological disasters occurring is 99.3%, and the amount of information provided is 1.93. Areas with weak engineering activities accounted for 62.5% of the total grid in the study area, the proportion of geological disasters that occurred was 0.7%, and the amount of information provided was − 6.88, which is generally not conducive to the occurrence of geological disasters.

Result 2 Comparison of susceptibility zoning and actual disaster distribution

GIS is used to perform grid coverage analysis on the weighted information amount of each impact factor to obtain a weighted information amount distribution map and reclassify it at equal intervals. Finally, the study area is divided into four levels: high-probability-prone areas, medium-probability-prone areas, low-probability-prone areas and non-prone areas. Compare the obtained susceptibility zoning with the actual disaster distribution. The results are shown in Table 2.

As can be seen from Table 2, the susceptibility zoning in this area is highly related to the geological disasters that have occurred. With the increase in the vulnerability level, the actual disaster occurrence rate (i.e., the ratio of the disaster density in different vulnerability areas to the total disaster density in the study area) increased, and the proportion of high-probability and medium-probability-prone areas was as high as 91.87%. The results show that the evaluation results are in good agreement with the actual disaster occurrence.

Result 3 Assessment of the susceptibility of geological disasters

Table 2 Comparison of susceptibility zoning and actual disaster distribution

Zone	Number of grids	Percentage of grids in this class of susceptibility to total grids (%)	Number of disasters falling in this vulnerable zone	Percentage of total disasters that occurred in this vulnerability zone (%)
Less prone to disaster	87,602	4.384	0	0
Low probability prone to disaster	675,163	33.785	10	8.13
Medium probability prone to disaster	996,528	49.866	51	41.463
High probability prone to disaster	239,641	11.965	62	50.407
Total	1,998,394	100	123	100

In order to further determine the validity of the results of the susceptibility to geological disasters, a quantitative test was performed using the receiver operating characteristic curve, and the area under the curve (AUC) was used to evaluate the accuracy of the model. The ROC curve is a diagonal line from the origin to the upper right corner, that is, the line segment (0, 0) to (1, 1). This line is called the diagonal of chance. If the obtained ROC curve falls on the diagonal of the opportunity, its AUC = 0.5. Generally, when the area under the curve is greater than 0.5, the closer the area under the curve is to 1, the better the accuracy of the model. When the area under the curve is 0.5–0.7, the accuracy is poor, and when the area under the curve is 0.7–0.9, the accuracy is better. The area under the curve is higher than 0.9, which means the accuracy is very good. In this paper, the percentage of the cumulative grid and total grid in the area from high to low information is used as the horizontal axis, and the percentage of cumulative grid and total grid of geological hazards in the corresponding information interval is used as the vertical axis. Get a curve passing through (0, 0), (1, 1), as shown in Fig. 7. The area under the curve is 87.3%, which indicates that the effectiveness of the method proposed in this paper is relatively high.

Result 4 The accuracy of BP neural network model training

Here we focus on the correct rate of BP neural network model training to provide a reference for the improvement of later work. In the course of the experiment, after normalizing the data, network training sample data was obtained. The sample data of each grid is trained 1000 times, and the weight matrix obtained after each training of each grid is tested for correctness. The average results of the accuracy of all grid tests are shown in Fig. 8.

It can be known from Fig. 8 that the accuracy of the model training fluctuates to different degrees at different stages. As the number of trainings increases, the accuracy of the grid weight matrix prediction tends to rise as a whole, and after the number of trainings is higher than 60, the fluctuation of its accuracy is getting smaller and smaller. In the end, the correct rate of BP neural network model training reached about 90%. The results of geological hazard risk classification are also highly consistent

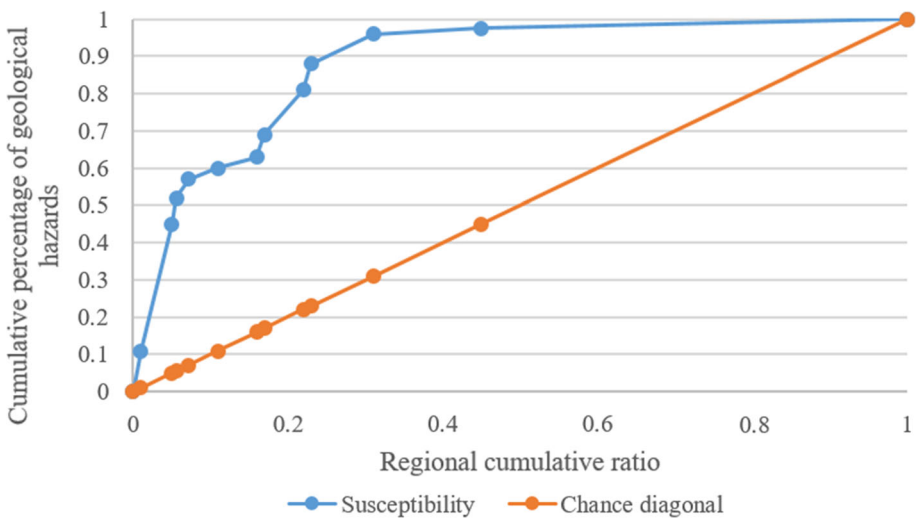

Fig. 7 ROC chart of geohazard disaster susceptibility evaluation results

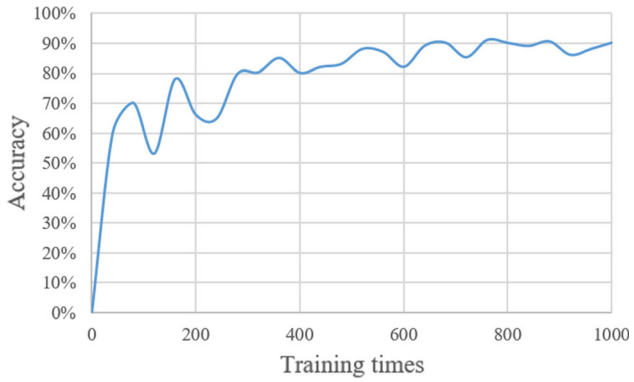

Fig. 8 Changes in the accuracy of BP neural network model training with the number of trainings

with the output of the network, indicating that they can be used to predict the geohazard hazard.

5 Conclusions

This article creatively combines the artificial neural network and GIS technology to apply to the study of geological disaster risk zoning. Make full use of basic geological data to facilitate the application of BP neural network in artificial neural network. It is worth mentioning that the method of combining artificial neural network and GIS technology has greatly enriched the connotation of GIS application in geological disaster prevention, and made the role of GIS change from pure data management to provide decision support for geological disasters.

Of course, due to the constraints of time and experimental equipment, in this article, only the combination of GIS and BP neural network in artificial neural network is discussed. In fact, other mathematical models can be added for comparison to make the results more accurate. In addition, in the study of geological disaster danger zoning, automation and intelligent division are also a future research direction, which needs further research.

Acknowledgements This work was supported by National Key R&D Plan of China (2018YFC1505505). This work was supported by SKLGP2015K016. (General Foundation Project at State Key Laboratory of Geo-hazard Prevention and Geo-environment Protection: Study on the mechanism of rock mass damage and instability during freezing and thawing in cold alpine mountainous regions); Ministry of Transport Technology Demonstration Project (2016009), Ministry of Transport Technology Demonstration Project (2016010), Sino-Ukrainian Science and Technology Exchange Project (CU03-32).

Compliance with ethical standards

Conflict of interest These are no potential competing interests in our paper. And all authors have seen the manuscript and approved to submit to your journal. We confirm that the content of the manuscript has not been published or submitted for publication elsewhere.

References

1. Pan YY, Zhao X, Cui XL (2017) Study about construction of sea ice disaster loss chain and assessment of indirect economic losses. Chin Fish Econ 35(1):95–100
2. Schindler M, Dorn RI (2017) Coatings on rocks and minerals: the interface between the lithosphere and the biosphere, hydrosphere, and atmosphere. Elem Int Mag Mineral Geochem Petrol 13(3):155–158
3. Savchenko IF, Belozerov NI, Girenko IV (2018) Geophysical processes, solar energy, and biosphere as system factors of the evolution of the earth. Izvestiya Atmos Ocean Phys 54(7):678–687
4. Xu D, Peng L, Liu S, Su C, Wang X, Chen T (2017) Influences of sense of place on farming households' relocation willingness in areas threatened by geological disasters: evidence from China. Int J Disaster Risk Sci 8(1):16–32
5. Noy I, duPont IV W (2018) The long-term consequences of disasters: what do we know, and what we still don't. Int Rev Environ Resour Econ 12(4):325–354
6. Kaur H, Gupta S, Parkash S (2017) Comparative evaluation of various approaches for landslide hazard zoning: a critical review in Indian perspectives. Spatial Inf Res 25(3):389–398
7. Menier D, Mathew M, Pubellier M, Sapin F, Delcaillau B, Siddiqui N, Ramkumar M, Santosh M (2017) Landscape response to progressive tectonic and climatic forcing in NW Borneo: implications for geological and geomorphic controls on flood hazard. Sci Rep 7(1):457
8. Alvarez L, Lindholm C, Villalón M (2017) Seismic hazard for Cuba: a new approach seismic hazard for Cuba: a new approach. Bull Seismol Soc Am 107(1):229–239
9. Du G, Zhang Y, Yang Z, Iqbal J, Tong B, Guo C, Yao X, Wu R (2017) Estimation of seismic landslide Hazard in the eastern Himalayan Syntaxis region of Tibetan plateau. Acta Geol Sin Engl Ed 91(2):658–668
10. Liu X, Miao C (2018) Large-scale assessment of landslide hazard, vulnerability and risk in China. Geomat Nat Hazards Risk 9(1):1037–1052
11. Abdallah C, Faour G (2017) Landslide hazard mapping of Ibrahim River Basin, Lebanon. Nat Hazards 85(1):237–266
12. Cipta A, Robiana R, Griffin JD, Horspool N, Hidayati S, Cummins PR (2017) A probabilistic seismic hazard assessment for Sulawesi, Indonesia. Geol Soc Lond Spec Publ 441(1):133–152
13. Bagheri V, Uromeihy A, Razifard M (2017) Evaluation of MLP and RBF methods for hazard zonation of landslides triggered by the Twin Ahar-Varzeghan earthquakes. Geotech Geol Eng 35(5):2163–2190
14. Hamza T, Raghuvanshi TK (2017) GIS based landslide hazard evaluation and zonation—a case from Jeldu District, Central Ethiopia. J King Saud Univ Sci 29(2):151–165
15. Ivanik O, Shevchuk V, Kravchenko D, Shpyrko S, Yanchenko V, Gadiatska K (2019) Geological and geomorphological factors of natural hazards in ukrainian carpathians. J Ecol Eng 20(4):177–186
16. Azimi SR, Nikraz H, Yazdani-Chamzini A (2018) Landslide risk assessment by using a new combination model based on a fuzzy inference system method. KSCE J Civ Eng 22(11):4263–4271
17. Nami MH, Jaafari A, Fallah M, Nabiuni S (2018) Spatial prediction of wildfire probability in the Hyrcanian ecoregion using evidential belief function model and GIS. Int J Environ Sci Technol 15(2):373–384
18. Rem BS, Käming N, Tarnowski M, Asteria L, Fläschner N, Becker C, Sengstock K, Weitenberg C (2019) Identifying quantum phase transitions using artificial neural networks on experimental data. Nat Phys 15(9):917–920

19. Carleo G, Troyer M (2017) Solving the quantum many-body problem with artificial neural networks. Science 355(6325):602–606
20. Chen M, Challita U, Saad W, Yin C, Debbah M (2019) Artificial neural networks-based machine learning for wireless networks: a tutorial. IEEE Commun Surv Tutor 21(4):3039–3071
21. Gonzalez-Fernandez I, Iglesias-Otero MA, Esteki M, Moldes OA, Mejuto JC, Simal-Gandara J (2019) A critical review on the use of artificial neural networks in olive oil production, characterization and authentication. Crit Rev Food Sci Nutr 59(12):1913–1926
22. Babu DJ, King P, Kumar YP (2019) Optimization of Cu(II) biosorption onto sea urchin test using response surface methodology and artificial neural networks. Int J Environ Sci Technol 16(4):1885–1896
23. Rajalingham R, Issa EB, Bashivan P, Kar K, Schmidt K, DiCarlo JJ (2018) Large-scale, high-resolution comparison of the core visual object recognition behavior of humans, monkeys, and state-of-the-art deep artificial neural networks. J Neurosci 38(33):7255–7269
24. Heriz HH, Salah HM, Abdu SBA, El Sbihi MM, Abu-Naser SS (2018) English alphabet prediction using artificial neural networks. Int J Acad Pedagog Res (IJAPR) 2(11):8–14
25. Chakraborty T, Chattopadhyay S, Chakraborty AK (2018) A novel hybridization of classification trees and artificial neural networks for selection of students in a business school. Opsearch 55(2):434–446
26. Mathioulakis E, Panaras G, Belessiotis V (2018) Artificial neural networks for the performance prediction of heat pump hot water heaters. Int J Sustain Energ 37(2):173–192
27. Kuo PH, Huang CJ (2018) A high precision artificial neural networks model for short-term energy load forecasting. Energies 11(1):213
28. Murphy MC, Manduca A, Trzasko JD, Glaser KJ, Huston J III, Ehman RL (2018) Artificial neural networks for stiffness estimation in magnetic resonance elastography. Magn Reson Med 80(1):351–360

Publisher's Note Springer Nature remains neutral with regard to jurisdictional claims in published maps and institutional affiliations.